Molecular Biology of the Cell
Vol. 11, 2497–2511, July 2000

Entry of the Two Infectious Forms of Vaccinia Virus at the Plasma Membane Is Signaling-Dependent for the IMV but Not the EEV

Jacomine Krijnse Locker,*§ Annett Kuehn,* Sibylle Schleich,* Gaby Rutter,† Heinrich Hohenberg,† Roger Wepf,‡ and Gareth Griffiths*

*European Molecular Biology Laboratory, Meyerhofstrasse 1, 69117 Heidelberg, Germany; †Heinrich Pette Institute, Martinistrasse 52, 2000 Hamburg, Germany; and ‡Beiersdorfs AG, Unnastrasse 48, 20245 Hamburg, Germany

Submitted April 11, 2000; Revised May 8, 2000; Accepted May 10, 2000
Monitoring Editor: Suzanne R. Pfeffer

The simpler of the two infectious forms of vaccinia virus, the intracellular mature virus (IMV) is known to infect cells less efficiently than the extracellular enveloped virus (EEV), which is surrounded by an additional, TGN-derived membrane. We show here that when the IMV binds HeLa cells, it activates a signaling cascade that is regulated by the GTPase rac1 and rhoA, ezrin, and both tyrosine and protein kinase C phosphorylation. These cascades are linked to the formation of actin and ezrin containing protrusions at the plasma membrane that seem to be essential for the entry of IMV cores. The identical cores of the EEV also appear to enter at the cell surface, but surprisingly, without the need for signaling and actin/membrane rearrangements. Thus, in addition to its known role in wrapping the IMV and the formation of intracellular actin comets, the membrane of the EEV seems to have evolved the capacity to enter cells silently, without a need for signaling.

INTRODUCTION

Vaccinia virus (vv), the best studied member of the poxvirus family, contains a dsDNA genome of 190-kB encoding for over 200 proteins, of which ~100 (Essani and Dales, 1979) make up the roughly brick-shaped particle, 350 × 250 nm in size. Poxviruses are unique in several respects. First, transcription as well as DNA replication occur in the host–cell cytoplasm, since the proteins required for both processes are encoded for in the viral genome. Second, during the assembly of vv, two infectious forms are made: the intracellular mature virus (IMV) and the extracellular enveloped virus (EEV; Moss, 1990). Both particles enclose an identical DNA-containing core (see below).

The assembly of vv starts at 5–6 h after infection with the formation of crescent-shaped membranes modified by viral membrane proteins. These membranes are derived from the intermediate compartment and consist of two tightly apposed cisternal membranes (Sodeik *et al.*, 1993; Rodriguez *et al.*, 1995; Wolffe *et al.*, 1996; for a different interpretation see Hollinshead *et al.*, 1999). The cisternal crescents form spherical particles, the so-called immature viruses that contain in their central part the viral core proteins (Ericsson *et al.*, 1995; Cudmore *et al.*, 1996). When the immature viruses take up the DNA, the particle undergoes a complex series of morphological changes to form the brick-shaped IMV. It is generally believed that the IMV remains intracellularly and is released only on cell lysis. A small percentage of the IMVs (5–20%, depending on the host cell) becomes enwrapped by a membrane cisterna derived from the trans-Golgi network (Schmelz *et al.*, 1994) to form the so-called intracellular enveloped virus, that exploits the actin cytoskeleton to propel itself through the cell toward the plasma membrane (Cudmore *et al.*, 1995). The outer membrane surrounding the intracellular enveloped virus then fuses with the plasma membrane to release the EEV into the extracellular space. The EEV thus contains the underlying IMV surrounded by an additional membrane with a unique set of (six identified) EEV-specific membrane proteins (Payne, 1978; see Roper *et al.*, 1996 and references therein). Functional as well as genetic studies have shown that the EEV is required for efficient cell-to-cell spread of the virus (Payne, 1980; Blasco and Moss, 1991). In addition, its entry appears to be faster and more efficient than that of the IMV (Payne and Norrby, 1978; Doms *et al.*, 1990), making it well suited for rapid dissemination.

The entry of enveloped viruses generally occurs in two possible ways. On receptor binding, the viral envelope can either fuse directly with the plasma membrane or, alterna-

§ Corresponding author. Email address: Krijnse@EMBL-Heidelberg.DE.

tively, the particle is internalized to reach endosomes where a low pH-induced fusion occurs (for reviews, see Marsh and Helenius, 1989; Kielian and Jungerwirth, 1990). Whether the viral membrane fuses with the plasma or the endosomal membrane, the final result of this process is the delivery of the viral genome-containing core to the cytoplasm of the host cell.

The entry of larger particles such as intracellular bacteria into mammalian cells generally involves phagocytosis. The interaction of the pathogen with the cell surface induces a complex signaling cascade, leading to actin rearrangements at the plasma membrane to form a phagocytic cup that engulfs the bacterium (Dramsi and Cossart, 1998). Signaling cascades responsible for actin rearrangements at the plasma membrane on bacterial entry are only partially understood (Galan, 1996; Menard *et al.*, 1996; Finlay and Cossart, 1997; Dramsi and Cossart, 1998), and in some cases GTPases of the rho family, which are known to control actin dynamics and achitecture (Hall, 1998), have been shown to play a role (Adam *et al.*, 1996; Chen *et al.*, 1996; Watarai *et al.*, 1997; Hauck *et al.*, 1998; Mounier *et al.*, 1999). In contrast, little is known about a possible relationship between the entry of enveloped viruses and actin. The few available studies suggesting such a relationship were restricted to showing that the entry of some enveloped viruses may be affected by actin-depolymerizing drugs (Rosenthal *et al.*, 1985; Gottlieb *et al.*, 1993; Kizhatil and Albritton, 1997; Iyengar *et al.*, 1998; Vanderplasschen *et al.*, 1998).

The data concerning poxvirus entry are controversial. It has been suggested from EM studies that vv may enter by phagocytosis (Dales and Kajioka, 1964) or by fusion at the plasma membrane (Armstrong *et al.*, 1973; Chang and Metz, 1976) and at neutral pH (Doms *et al.*, 1990). Observations by Payne and Norrby (1978) suggested that the entry of the IMV may require actin since it was inhibited by cytochalasin B, while the EEV entry was unaffected by this drug. More recent data, however, suggested that the entry of both the IMV and the EEV is sensitive to cytochalasin D (Vanderplasschen *et al.*, 1998).

In this article, we have tried to resolve some of these contradictory results. We show, that although the (identical) cores of both the IMV and the EEV enter at the plasma membrane into the adjacent cytoplasm, IMV entry requires actin dynamics, while the EEV does not. In addition, the IMV, but not the EEV, induces a signaling cascade from which we identify a number of key players, including the actin-binding protein ezrin, tyrosine, as well as protein kinase C phosphorylation and the small GTPase rac1. These signaling events appear to stimulate the assembly of actin/membrane protrusions that seem to be required for efficient IMV entry.

MATERIALS AND METHODS

Materials

All chemicals were from Calbiochem (San Diego, CA) except for cytochalasin D (CD), taxol, sphingosine 1-phosphate (S 1-P), and staurosporin (Sigma, St. Louis, MO) and latrunculin A (Lan A) and jasplakinolide (Jasp; Molecular Probes, Eugene, OR)

Cells and Virus Preparation

HeLa cells (clone CCL3; ATTC, Manassa, VA) and RK13 cells were grown as described (Sodeik *et al.*, 1993). Purified IMV (strain IHD-J) was prepared as before (Jensen *et al.*, 1996), except that the virus was purified on a 22–32% OptiPrep (Nycomed, GIBCO BRL, Grand Island, NY) gradient in 10 mM Tris-Cl, pH 9, that was run for 45 min at 24,000 rpm in a SW27 rotor. EEV preparations were obtained by infecting monolayers of confluent RK13 cells at a multiplicity of infection (MOI) of 50 for 2 h at 37°C, after which the inoculum was replaced by serum-free DMEM. The virus was concentrated from the culture medium that was harvested 24 h later, by centrifugation for 30 min at 24,000 rpm in a SW27 rotor. The pelleted virus was purified on OptiPrep gradients as described for the IMV. IMV and EEV preparations banded in OptiPrep gradients were harvested, snap-frozen in liquid nitrogen, and kept at −80°C. Pfu per particles ratios were calculated as described in Pedersen *et al.* (2000). Briefly, the titer was determined by plaque assay, and the number of particles was determined by OD_{260} measurement. As for IMV and EEV purified on sucrose gradients the pfu/particles ratios for OptiPrep-purified IMV and EEV preparations were 1:50 and 1:15, respectively. These ratios are comparable to those obtained by Vanderplasschen and Smith (1997) using purified IMV or EEV taken directly from the culture medium.

Antibodies and Plasmids

The anticore, antip16 (gene *A14L*) antibodies and the monoclonal antibody to the EEV membrane protein p42 (gene *B5R*) have been described before (Schmelz *et al.*, 1994; Salmons *et al.*, 1997; Krijnse Locker and Griffiths, 1999). Monoclonal antibodies to VSV-G P5D4- and to *myc*-epitope were provided by Alan Sawyer. Antiezrin, moesin, and radixin antibodies were from Paul Mangeat, and antiactin antibody was from Dr. Gabianni. Antibodies to rac1 were from Transduction Laboratories (Lexington, KY 40511-2624). P5D4-tagged full-length ezrin or ezrin 1–309 in pCB6 were a gift of Dr. Monique Arpin (Algrain *et al.*, 1993). *Myc*-tagged V14RhoA and N19RhoA in pCDNA3 were a gift of Dr. T. Jacks (Shaw *et al.*, 1998), and *myc*-tagged N17rac1 and L61rac1 in pRK5 as well as N17CDC42 and L61CDC42 in pRK3 were obtained from Dr. A. Hall. The plasmid expressing rac1-GTP binding domain of pak3 fused to GST (PBD-GST) was a gift of Shubha Bagrodia and Becky Worthylake (Bagrodia *et al.*, 1998).

Biochemical Binding and Entry Assay

HeLa cells plated in 10 cm^2 dished at a density of 4×10^5cells per dish were rinsed with cold serum-free DMEM (SFM) containing 20 mM HEPES and were cooled for 10 min on ice, before applying 100 000 cpm (corresponding to an MOI of ~10) of ^{35}methionine-labeled (Jensen *et al.*, 1996) IMV or EEV diluted in SFM (0.8 ml of diluted virus per dish). After binding for 60 min on ice, the cells were washed twice with PBS with 5 mM $CaCl_2$ and 8 mM $MgCl_2$, were overlayed with DMEM prewarmed at 37°C, and were incubated for the indicated times at 37°C. The cells were washed twice with ice-cold PBS containing 5 mM EDTA and EGTA and were incubated for 60 min on ice with 0.2 mg/ml trypsin (Sigma) in PBS/EGTA/EDTA. Aprotinin (Sigma) was added to a final concentration of 4 μg/ml, the cells were gently squirted off the dish, pelleted, and washed three times with PBS/EDTA/EGTA/aprotinin. Supernatant and washes were combined, the pellet was resuspended in 1 ml of PBS, and the radioactivity was determined by liquid scintillation counting. The percentage of entry was calculated by dividing the counts associated with the pellet by the total number of counts.

IF Entry Assay

HeLa cells plated in 24-well plates (2.5 cm^2 surface) with 11-mm diameter round coverslips at a density of 7×10^4 cells/well, were rinsed once with cold SFM/HEPES and were incubated for 10 min

in cold SFM/HEPES at room temperature. IMV and EEV preparations were diluted in SFM/HEPES (0.35 ml/well) at the indicated MOI. Diluted IMV was sonicated for 1 min in a waterbath sonicator, while the EEV was not sonicated. The cells were incubated for 60 min at room temperature to synchonize entry and then were switched to 37°C. At the indicated times, the cells were rinsed once with PBS and were fixed for 30 min at RT with 3% paraformaldehyde in PBS. Indirect immunofluorescence was performed as described (Den Boon *et al.*, 1991) using the anticore antibody at a dilution of 1:1000 and donkey antirabbit FITC (Dianova, Hamburg, Germany). Because ATCC HeLa cells CCL3 are quite variable in size, for quantitation of intracellular cores in each case 15 "big" and 15 "small" cells were counted.

Transfections

HeLa cells were plated in 10 cm^2 dishes containing six 11-mm diameter coverslips. Cells were transfected for 8 h at 37°C using calcium–phosphate precipitation, after which the cells were rinsed extensively with PBS and incubated overnight at 37°C. IF entry experiments on transfected cells were performed at 27–28 h post-transfection. After fixing, the cells were double labeled with antimyc or anti-P5D4 monoclonal antibodies and the anticore antibody.

Drug Treatments

The effect of different drugs on entry was tested by preincubating cells for 15 min at 37°C with the drugs at the indicated concentrations before the virus was allowed to bind at room temperature and to enter at 37°C in the presence of the drugs. The effects of S 1-P, PDGF, EGF, bradykinine, and bombesin were tested on HeLa cells that were serum starved for 24 h. The cells then were incubated for 10 min at 37°C with the respective compounds, after which binding and entry were performed in their presence.

Rac1 Activity Assay

Rac1 activity assay was performed as described (Waterman-Storer *et al.*, 1999). HeLa cells grown in 25-cm^2 dishes were washed once with warm serum-free DMEM and were incubated for the indicated times with purified IMV or EEV diluted in the same medium at an MOI of 40. The incubations were performed such that all dishes were lysed at the same time. Activated rac1 was affinity precipitated from cell lysates using PBD-GST (the rac1-GTP binding domain of pak3) coupled to GST-beads (Pharmacia, Uppsala, Sweden). Rac1-GTP was detected by Western blots using antirac1 monoclonal antibody at a dilution of 1:1000 and either goat antimouse-HRP (Bio-Rad, Richmond, CA) followed by ECL (Amersham, Arlington Heights, IL) or ^{35}SLR-labeled antimouse Ig (Amersham). The latter case was used to quantified rac1 GTP by phosphoimager.

Electron Microscopy, Surface Replica, and Cryoscanning EM

HeLa cells infected for 30 min with IMV or for 10 min with EEV at an MOI of 200 were fixed and prepared for cryosectioning as described (van der Meer *et al.*, 1999). For pre-embedding labeling followed by epon embedding, infected cells were fixed for 10 min at RT by the addition of an equal volume of 8% paraformaldehyde in 2× PHEM buffer (van der Meer *et al.*, 1999) to the culture medium. The labeling was done by a 1-h incubation at 4°C with an anti-vv antibody, followed protein gold. After extensive washing, the cells were postfixed for 30 min at RT with 1% glutaraldehyde in PBS and were embedded in epon as described (Ericsson *et al.*, 1995). For the surface replicas, HeLa cells were grown for 2 d on coverslips infected for 30 min at 37°C with IMV at an MOI of 50, were fixed, and were prepared for surface replica as described (Hohenberg, 1989). Cryoscanning-EM of unfixed infected HeLa cells were grown on carbon-coated sapphire disks, infected at an MOI of 50 for 30 min at 37°C, after which the cells were plunged frozen into liquid nitrogen. Samples were prepared and viewed as described by Ritter *et al.* (1999).

RESULTS

The Preparation of Purified Virion Preparations

Throughout this study, we used the IHD-J strain of vv that, when isolated from infected RK-13 cells, results in high yields of EEV in the extracellular medium (see Materials and Methods). Qualitative and quantitive viral entry studies require the preparation of highly purified and nonaggregated virus stocks. We chose to use OptiPrep gradients for the purification of IMV and EEV since several studies have shown Ioxidanol to be superior to sucrose for purifying intracellular organelles. The virion-containing band harvested from such gradients with a titer of $1–5 \times 10^8$ pfu/ml was used for all subsequent experiments. By negative staining EM, this fraction contained single virus particles with no cellular contamination (Figure 1, A and B). To document this latter point even further, the proteins contained in the virus bands obtained from sucrose or OptiPrep gradients were run on gels that were subsequently silver stained (Figure 1C). The protein pattern of sucrose or OptiPrep IMV and EEV preparations was completely identical with the EEV containing two additional prominent bands around 30 kDa (Figure 1C). These data show that OptiPrep gradients result in the same purified virus preparations as sucrose gradients, but that the former has the advantage that it can be used to infect cells directly without dialysis.

Two Quantitative Entry Assays

As illustrated in Table 1 and Table 2, we found that the binding of both the IMV and the EEV to HeLa cells was very poor. No more than 4% of the total viruses were bound after 1 h of absorption, and this poor binding appeared to vary little with the multiplicity of infection (MOI; Table 1) or temperature (Table 2) used. Similar poor binding also was observed in the study by Vanderplasschen and Smith (1997), who used confocal microscopy to study vv binding. Although the binding efficiency was not calculated or mentioned in that study, their results infer that at an MOI of 5 to 10 and no more than 2.4% of the total particles from sucrose-purified IMV or EEV bound after 60 min on ice to HeLa, RK13, and BSC-40 cells.

The first assay consisted of binding ^{35}S-methionine-labeled purified virions to HeLa cells on ice, washing away unbound viruses and allowing entry to occur at 37°C. Since the (poor) binding appeared independent of the MOI, we used a constant amount of radioactivity for binding (100 000 cpm, corresponding in fact for most virus preparations to an MOI of ~10) rather than a constant number of infectious particles. At each time point of interest, the unpenetrated virions at the plasma membrane were removed by a trypsin treatment on ice, resulting in two radioactive values: cell-associated (trypsin protected) and non-cell–associated counts. The percentage of virus entry was calculated by dividing the cell-associated counts by the total counts.

IMV entry was relatively slow and inefficient (Figure 2A). About 45% of the bound virus entered over a 1-h period, while this was 60–70% for the EEV. In the case of the IMV,

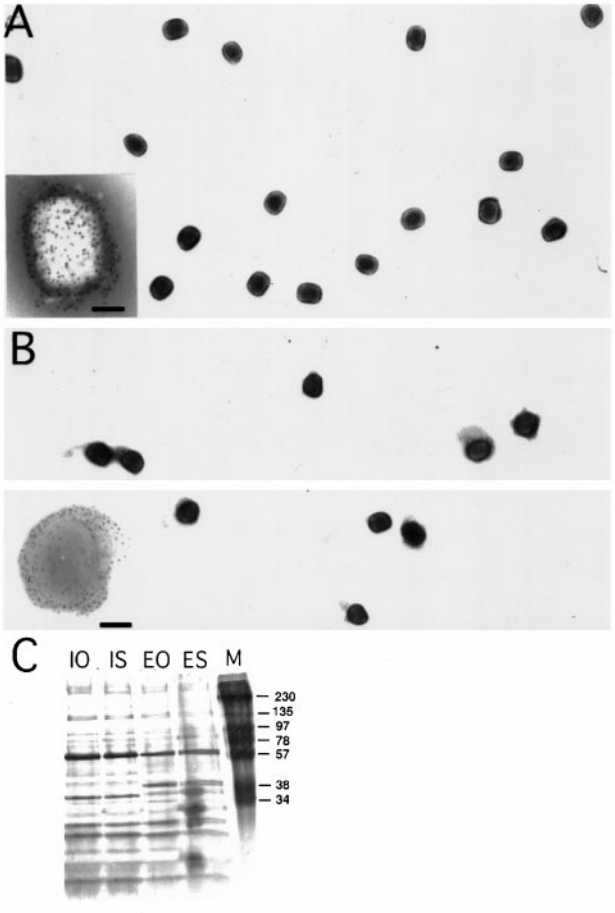

Figure 1. Negative staining EM and silver-stained gels of OptiPrep and sucrose-purified IMV and EEV preparations. OptiPrep-purified IMV (A) and EEV (B) preparations were absorbed to formvar/carbon-coated grids and were stained with 2% ammonium molybdate. The insets at the bottom left show labeling with antibodies to surface antigens of the IMV (p14 gene A27L) in (A) and EEV (p42; gene *B5R*) in (B). The bar in the insets is 100 nm. Note that during negative staining using ammonium molybdate the EEV-specific membrane in B tends to collapse on the grid. In (C) sucrose-purified and OptiPrep gradient-purified IMV and EEV preparations were run on 15% SDS-PAGE, and the proteins were detected by silver staining. IO, OptiPrep-purified IMV; IS, sucrose-purified IMV; EO, optiprep-EEV; ES, sucrose-purified EEV; M, marker.

half of the total amount that was cell associated after 1 h entered in 30 min, while for the EEV this took only 11 min. These data are consistent with previous results (Doms *et al.*, 1990), showing that the entry of the IMV was slower and less efficient than that of the EEV. Moreover, the data show that our virus preparations have distinct entry kinetics/properties, validating our EEV and IMV purification procedures.

A second entry assay relied on an antibody against vv cores, which by immunofluorescence recognizes the vv cores only when these are in the cytosol following penetration (not shown; see also Vanderplasschen *et al.*, 1998). To synchronize entry, viruses were bound for 60 min at RT (a temperature at which no entry occurs, see Doms *et al.*, 1990).

Table 1. The binding of IMV and EEV at different multiplicities of infection and at 4°C[a]

	Percentage of binding			
	1 h	2 h	3 h	4 h
IMV				
MOI 1	1.9	2.7	4.6	4.2
MOI 5	2.0	3.5	3.1	7.8
MOI 10	1.6	2.4	1.6	4.9
EEV				
MOI 1	2.0	3.6	5.7	7.3
MOI 10	1.1	3.2	3.1	6.3
MOI 20	1.1	2.5	3.2	5.8

[a] 100 000 cpm of ^{35}S-labeled IMV or EEV preparations were bound for indicated times on ice to monolayers of HeLa cells. Percentage of binding was calculated by dividing the cell-associated counts by the total counts. The values are the average of duplicates and from two independent experiments.

Since even at that temperature the binding is poor, entry was subsequently allowed to occur at 37°C without removing viruses that remained unbound after the RT incubation period. At various times after infection, the cells were fixed and labeled with the anticore antibody, and the intracellular cores were counted.

Figure 2B shows such a time course. In agreement with the results using the ^{35}S-labeled virions, it took ~30 min for the IMV to reach half of the total amount of intracellular cores that we counted at 60 min of infection, while for the EEV this took around 20 min. In the case of the EEV (but not for the IMV), there was a significant variation in the number of intracellular cores found in different cells, most likely due to the fact that EEV preparations generally have a greater tendency to aggregate during the assay (unpublished observations). This may explain the

Table 2. The binding of IMV and EEV at different temperatures

	Percentage of binding[a]			
	1 h	2 h	3 h	4 h
IMV				
4°C	1.9	2.7	4.6	4.2
15°C	4.6	6.7	9.0	8.9
18°C	2.8	3.8	7.6	9.0
22°C	2.9	4.5	10.6	10.8
EEV				
4°C	2.0	3.6	5.7	7.3
15°C	4	4.8	7.0	7.9
18°C	3.4	3.2	5.9	9.3
22°C	3.1	8.9	12.8	17.7

[a] 100 000 cpm of ^{35}S-labeled IMV and EEV preparations were bound for the indicated times and indicated temperatures to monolayers of HeLa cells at a MOI of 1. Percentage of binding was calculated by dividing the cell-associated counts by the total counts. The values are the average of duplicates and from two independent experiments.

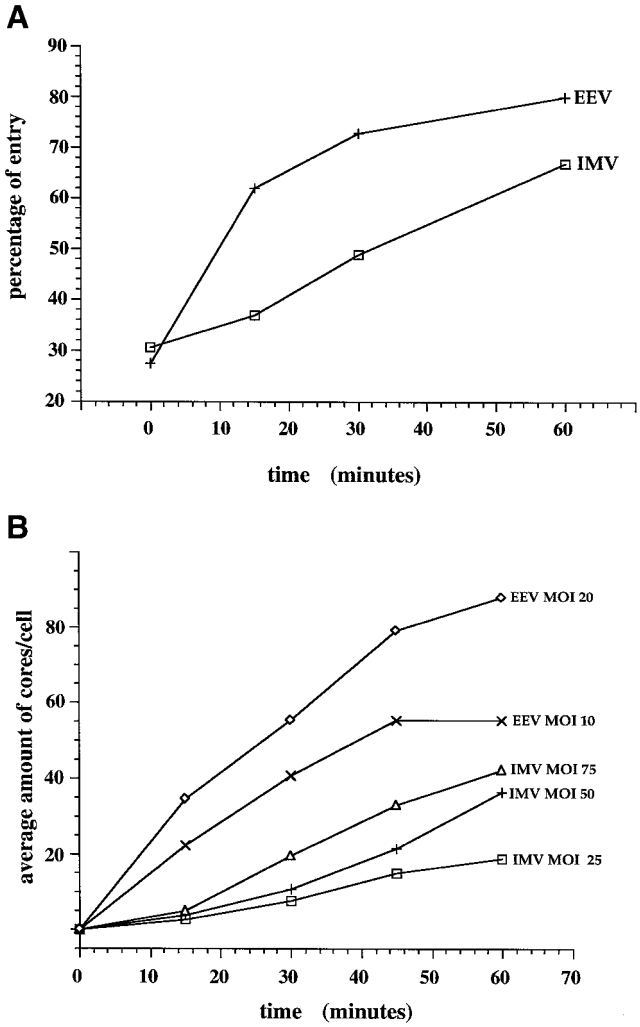

Figure 2. Establishment of two quantitative entry assays. (A) [^{35}S]methionine-labeled and -purified IMV or EEV (indicated) were bound and allowed to enter HeLa cells as described in Materials and Methods. At the indicated times, the cells were digested for 60 min on ice with 0.2 mg/ml of trypsin, and penetrated virus was separated from unpenetrated virus by pelleting the cells. The percentage of entry was calculated by dividing the cell-associated counts by the total counts (the addition of cell-associated and non-cell–associated cpm). The values are the average of duplicates. (B) Purified IMV or EEV preparations were bound for 60 min at RT to monolayers of HeLa cells at different MOIs. The cells were transferred to 37°C and were fixed after incubation at this temperature for the indicated times. Entry was determined by counting the average amount of intracellular cores per cell by immunofluorescence in 30 HeLa cells.

discrepancy between the "half-time" of EEV entry using the assay based on the penetration of ^{35}S-labeled virions versus this IF-assay.

Because of the relative ease of the IF entry assay, compared with the assay with ^{35}S-labeled virions, essentially all of the subsequent experiments were carried out using this assay.

Table 3. The effect of CD, Lan A, and Jasp on IMV and EEV entry

Concentration (μM)	CD[a]	%[b]	Lan A[a]	%	Jasp[a]	%
IMV						
0	70.5 ± 20.8	100	70.5 ± 20.8	100	70.5 ± 20.8	100
0.5	26.8 ± 10.9	38	17.3 ± 11.6	25	32.7 ± 14.1	46
1	19.4 ± 10.4	28	17.0 ± 11.3	24	27.7 ± 16.7	39
2	12.0 ± 5.9	17	10.4 ± 7.4	15	20.3 ± 11.4	29
4	ND[c]	ND	3.7 ± 4.9	5	13.6 ± 7.1	19
EEV						
0	68.2 ± 23.3	100	68.2 ± 23.3	100	68.2 ± 23.3	100
0.5	61.8 ± 29.4	91	59.6 ± 18.5	87	67.5 ± 25.4	99
1	66.2 ± 27.6	97	65.5 ± 25.0	96	72.8 ± 21.7	107
2	65.2 ± 29.0	96	67.9 ± 30.0	99	70.2 ± 26.9	103
4	63.5 ± 26.8	93	67.7 ± 25.0	99	59.0 ± 20.3	87

[a] Average number of cores and S.D.s per cell after infection with IMV at MOI 50 or at EEV at MOI 20 and after pretreatment with CD, Lan A, and Jasp at the indicated concentrations; $n = 30$. In each case, the number of cores in the cytoplasm of 15 "small" and 15 "big" HeLa cells were counted.

[b] Percentage of control, the average amount of cores in untreated cells was taken as 100%.

[c] ND, not done.

The Entry of the IMV Requires Actin-Dynamics

The role of the actin cytoskeleton in IMV and EEV entry was investigated next. HeLa cells were preincubated for 15 min at 37°C with drugs that affect actin-dynamics, after which the virus was bound and allowed to enter at 37°C in the presence of the drugs, and the intracellular cores were counted by IF. To affect actin-dynamics, we used CD, the most commonly used drug to block actin-assembly (Cooper, 1987), Lan A, which has been shown to be a powerful actin-depolymerizer (Ayscough, 1998), and Jasp, which binds F-actin and blocks actin-disassembly (Bubb *et al.*, 1994; Holzinger and Meindl, 1997). Control experiments using our HeLa cells confirmed the expected effects of the three drugs (not shown).

These three drugs were found to substantially affect the entry of the IMV; at a concentration of 0.5 μM, for instance,

Table 4. The effect of nocodazole and taxol on IMV and EEV entry

	IMV		EEV	
Treatment	No. of cores[a]	%[b]	No. of cores	%
Control[c]	59.5 ± 20.9	100	68.8 ± 23.3	100
Nocodazole (10 μM)	54.0 ± 20.0	91	69.1 ± 25.1	101
Taxol (2 μM)	61.5 ± 22.9	103	68.6 ± 25.4	101

[a] Average number of cores and S.D.s per cell after infection with IMV (MOI 50) or EEV (MOI 20); $n = 30$. In each case the amount of cores in the cytoplasm of 15 "small" and 15 "big" HeLa cells were counted.

[b] Percentage of control, the average amount of cores in untreated cells was taken as 100%.

[c] Control signifies no drug treatment.

CD inhibited IMV entry by 62%, Lan A by 75%, and Jasp by 54%, while this inhibition amounted to 83%, 85%, and 71%, respectively, at a concentration of 2 μM (Table 3). No such effect was observed when interfering with the microtubular network, since neither nocodazole (at 10 μM) nor taxol (at 2 μM) pretreatment of cells affected IMV or EEV entry (Table 4). Remarkably, however, none of these actin drugs affected the entry of the EEV (Table 3).

These data demonstrate that the IMV entry requires a dynamic actin-network, while EEV enters in an actin-independent manner, which is in agreement with the earlier experiments of Payne and Norrby (1978)

The IMV induces the formation of long actin/ezrin-containing protrusions, to which it binds and through which it may enter

When analyzing thawed cryosections of HeLa cells infected with IMV for 30 min, the cells showed an unusual amount of long "finger-like" protrusions at the plasma membrane (Figure 3). The labeling of thawed cryosections with antibodies to actin showed that the protrusions were clearly enriched in this cytoskeletal protein (Figure 3A). By indirect immunofluorescence, the protrusion not only were labeled with rhodamine phalloidin (actin; Figure 4C) but were also enriched in the actin-binding proteins ezrin (Figure 4D), moesin, and radixin (not shown). Uninfected cells (Figure 4, A and B) or cells exposed to EEV (not shown) did not show such long filopodia-like structures at the plasma membrane. Cryosections of infected HeLa cells confirmed the localization of ezrin to the (virus-induced) plasma membrane protrusions (Figure 3B).

Using a surface-replica technique as well as cryoscanning EM of unfixed preparations, the extent of the formation of these protrusion became very obvious (Figure 5). These two approaches showed that the entire surface of infected HeLa cells appeared covered with these projections, which often reached many microns in length (see e.g., Figure 5B), while uninfected cells or cells exposed to EEV never showed such dramatic numbers of protrusions (not shown).The IMVs had a clear affinity for these protrusions; most virions were found to be associated with them, while the smooth parts of the plasma membrane were practically devoid of particles (Figure 5).

Cryosections as well as plastic-embedded, infected HeLa cells were used subsequently to determine the fate of the IMVs that were bound to the filopodia. One option was that the protrusions enwrapped the IMVs, which was followed by phagocytosis of the whole (intact) virion. Alternatively, the virions just associated with the protrusions or used them for an entry mechanism distinct from phagocytosis. Figure 6 shows examples of whole virions that are on the outside of the cells and of cores that have entered the microvillar-like structures; in these representative images, the viral membrane remained at the cell surface (Figure 6B), while the core ended up "free" (not surrounded by any membrane organelle) in the cytoplasm. No whole particles were seen inside vacuolar organelles at these early times of infection.

Since the entry of the IMV core at the plasma membrane required actin-dynamics but EEV entry was actin-independent, we asked whether the latter virus entered in a different way, perhaps by means of endocytosis/phagocytosis. Cryosections prepared from cells that were infected for 10 min with EEV, however, showed many images of cores (identical to those derived from the IMV) penetrating into the cytoplasm at the plasma membrane, with no hint of whole, intact particles being internalized. Close to these cytoplasmic cores, viral membrane remnants were observed to be attached to the plasma membrane, which contained both EEV and IMV membrane proteins (Figure 6, F and G). While the precise mechanism of IMV and EEV entry is still under investigation, these data show that the core of both viruses penetrates into the cytoplasm at the plasma membrane in a way that at first glance resembles a fusion process (see Discussion), excluding phagocytosis or endocytosis as the entry pathway. Surprisingly, however, plasma membrane entry of the IMV required the induction of actin-containing protrusions through which at least a subset of the cores may enter, while EEV entry occurred without the need of filopodia formation at the cell surface.

Overexpression of the N-Terminal Half of Ezrin Increases IMV Entry

That the actin-binding protein ezrin was present in the virus-induced projections was not unexpected. Ezrin is a member of the so-called ERM (ezrin, radixin, and moesin) family of proteins that are found in ruffling membranes and microvilli, where they are thought to link the actin cytoskeleton to the plasma membrane (Tsukita and Yonemura, 1997; Bretscher, 1999; Mangeat *et al.*, 1999). Several studies have shown that the overexpression of truncated versions of ezrin interferes with its normal function. The overexpression of ezrin 1–310 or ezrin 310 to 586 in insect cells was shown to induce the formation of long protrusions at the plasma membrane (Martin *et al.*, 1995 and 1997). Similar effects were observed on overexpression of ezrin 1–310 in CHO and CV-1 cells (Algrain *et al.*, 1993). Overexpression of this same construct in LLC-PK1 cells, however, resulted in fewer microvilli on the surface of these cells (Crepaldi *et al.*, 1997; Skoudy *et al.*, 1999).

When expressing ezrin 1–309 in HeLa cells tagged with a VSV-G epitope, allowing the discrimination of transfected versus untransfected cells, the overexpressed protein was present in prominent protrusions, apparently induced by this construct. The overexpressed full-length molecule also was found in protrusions, but, compared with ezrin 1–309, significantly more of the overexpressing cells showed a more general cytosolic localization (data not shown). While the overexpression of full-length ezrin had no effect on IMV or EEV entry, the overexpression of the N-terminal fragment resulted in a 50% increase in the entry of the IMV compared with untransfected control cells (Table 5). EEV entry, however, was unaffected by the overexpression of ezrin 1–309 (Table 5).

These data show that interfering with ezrin function affects IMV entry, but not EEV entry.

The Role of Rho-GTPases in IMV and EEV Entry

ERM proteins are known to have complex interactions with different members of the rho-family GTPases (see Discussion). The relationship of these GTPases and actin rearrang-

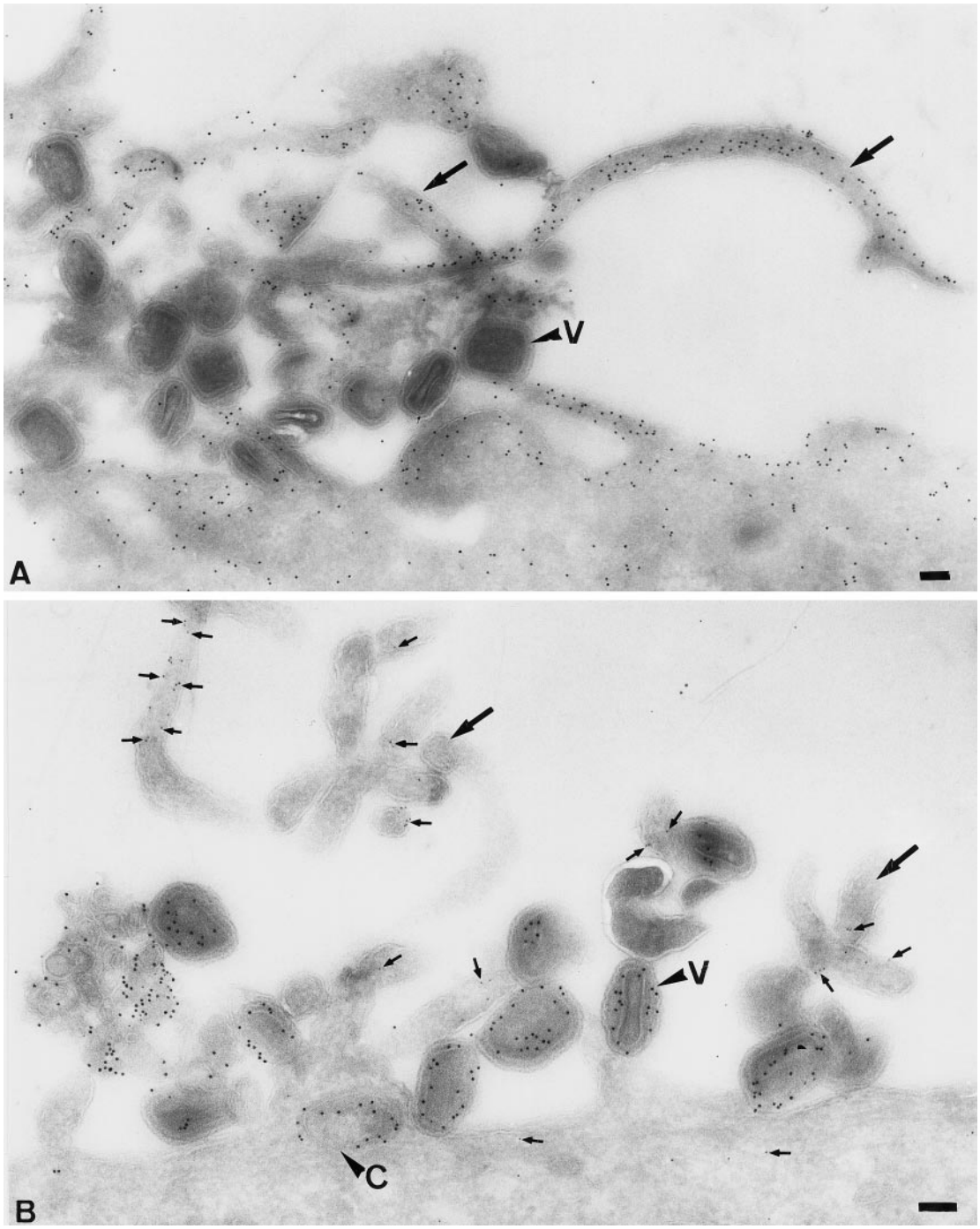

Figure 3. The exposure of HeLa cells to IMV results in the formation of long microvillar-like structures that contain actin and ezrin. HeLa cells were incubated for 30 min at 37°C with IMV at an MOI of 200. The cells were fixed, prepared for cryosectioning, and labeled with antibodies to actin (A) or were double labeled (B) with antiezrin (5-nm gold, *small arrows*) and anticore antibody (10-nm gold). *Large arrows* indicate typical IMV-induced protrusions. V, virions; C, core; bars, 100 nm.

ments has been well documented in mouse fibroblasts; RhoA is thought to be involved in stress fiber and focal adhesion assembly, while rac1 and CDC42 usually regulate the formation of lamellipodia and filopodia, respectively (Hall, 1998). The long protrusions induced at the plasma membrane by the IMV had all the hallmarks of slender filopodia, suggesting that CDC42 might be involved in their formation.

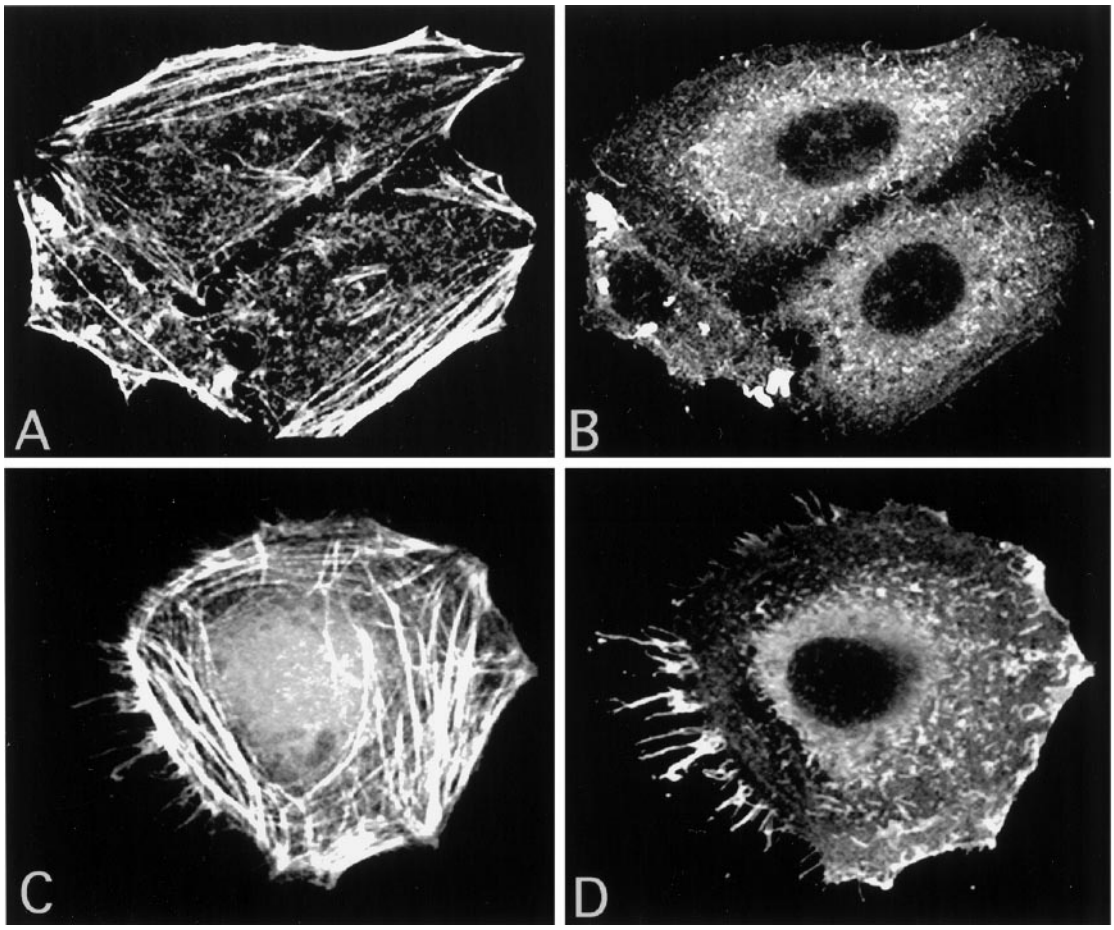

Figure 4. Localization of actin and ezrin by indirect immunofluorescence and confocal microscopy. The localization of actin (A) and ezrin (B) in uninfected HeLa cells is shown. In (C) and (D), HeLa cells were exposed for 10 min at 37°C to IMV at an MOI of 50. The picture in (C) is overexposed to show the labeling of rhodamine–phalloidin in the slender cell–surface projections induced by the virus.

To address the possible role of these GTPases in vv entry, HeLa cells were transiently transfected with *myc*-tagged versions of activated and dominant-negative rhoA, rac1, and CDC42 (G25K isoform) and were infected with either the IMV or the EEV. Table 5 shows that none of these overexpressed proteins had an effect on EEV entry, while three of them significantly affected IMV entry. Constitutively activated rhoA inhibited IMV entry by ~70%. Activated rac1, however, doubled the number of cores in the cytoplasm on infection with the IMV, relative to untransfected control cells, while the dominant-negative rac1 inhibited entry by ~45% (Table 5). Finally, the overexpression of activated or dominant-negative CDC42 had no effect on IMV entry, ruling out a likely role for this GTPase in the IMV entry (Table 5).

We then used a recently described assay to test directly whether the IMV was able to activate rac1; in this assay the rac1-GTP (or CDC42-GTP)-binding domain of pak3 fused to GST is used to affinity isolate rac1-GTP (but not Rac1-GDP) from cell lysates (Bagrodia *et al.*, 1998; Waterman-Storer *et al.*, 1999). Compared with uninfected cells, rac1-GTP levels in HeLa cells gradually increased up to 3.5-fold after 60 min when they were exposed to IMV (Figure 7). Consistently, no such rac1 activation was observed when using EEV (not shown).

Further evidence that rac1 activation might be implicated in IMV entry was obtained using specific ligands. The relationship between receptor activation and the activation of rho proteins has been studied in detail in serum starved Swiss 3T3 cells (see Zigmond, 1996 for a review).

HeLa cells were serum starved for 24 h and were exposed for 10 min to several of these ligands after which the effect on IMV and EEV entry was tested. Serum starvation of HeLa cells led to a 10% decrease in IMV entry compared with nondeprived cells, while EEV entry was not affected (not shown). Furthermore, we observed that serum starvation for longer than 24 h led to an almost complete block of IMV (but not EEV) entry. Upon treatment of serum-starved HeLa cells with several ligands known to activate rho proteins, EEV entry was again unaffected (Table 6). Consistent with the effect of activated rhoA on IMV, S 1-P, which has been linked to rhoA activation, inhibited IMV entry by ~70%. Bradykinin and platelet-derived growth factor (PDGF) had no effect on the IMV entry, while epidermal growth factor

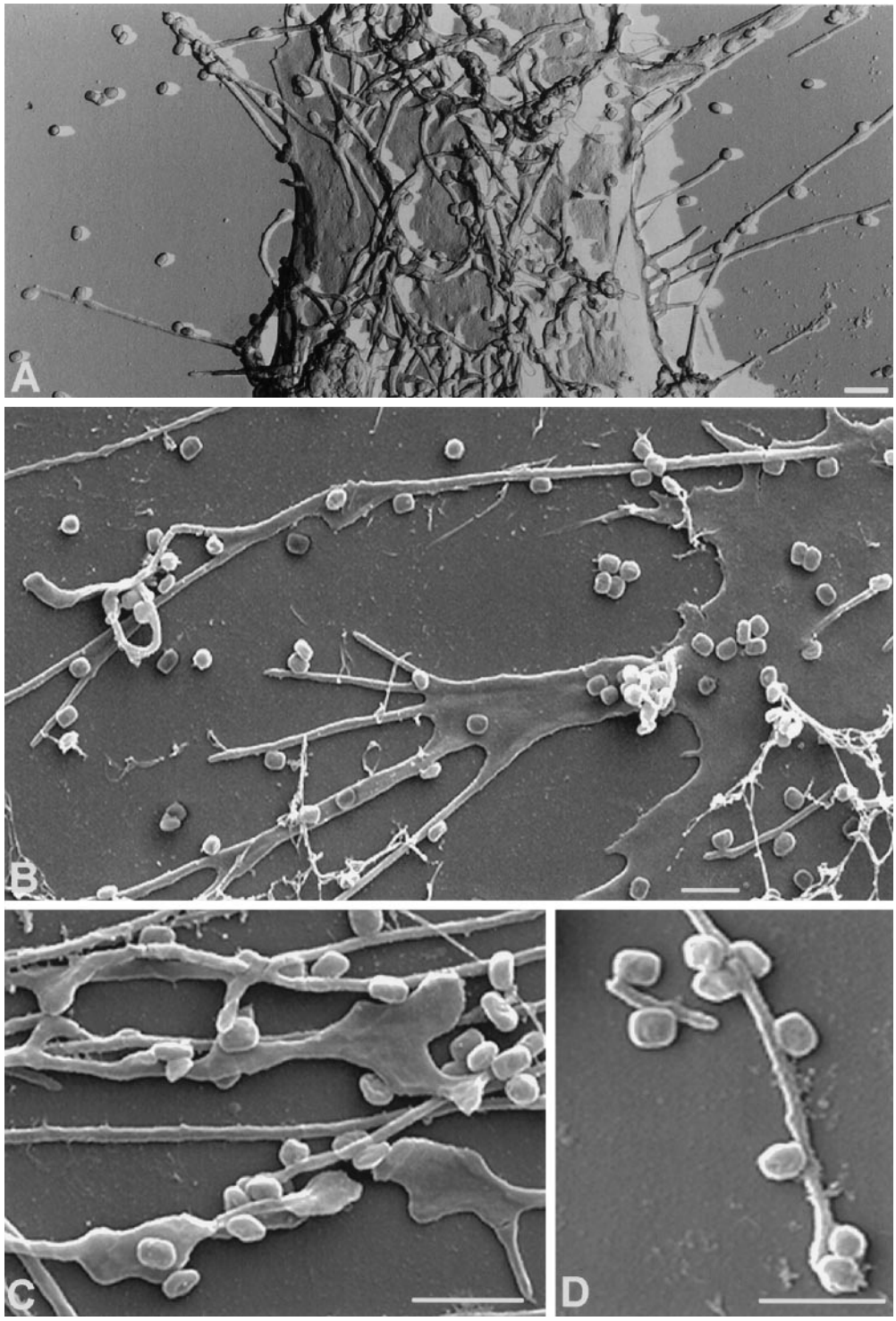

Figure 5. Replica (A) and cryoscanning EM (B–D) of the surface of IMV-infected HeLa cells. (A) The surface replica of HeLa cells infected for 30 min with IMV at a MOI of 50. There are many projections with bound virions projecting toward the eye that are more difficult to resolve. (B)–(D) Cryoscanning EM of HeLa cells infected for 15 min with IMV at an MOI of 50. (B) shows an overview of a cell that has responded to the IMV incubation by making a lamellipodium that branches in several thin projections. From the same cell another filopodia-like structure emanates that reached ~16 μm in size and to which many virions are bound. In (C) and (D), close-ups of several projections with bound IMVs, showing that in many instances the diameter of the virions (250 × 350 nm) exceeds the diameter of the induced microvillar-like structures. Bars, 1 μm.

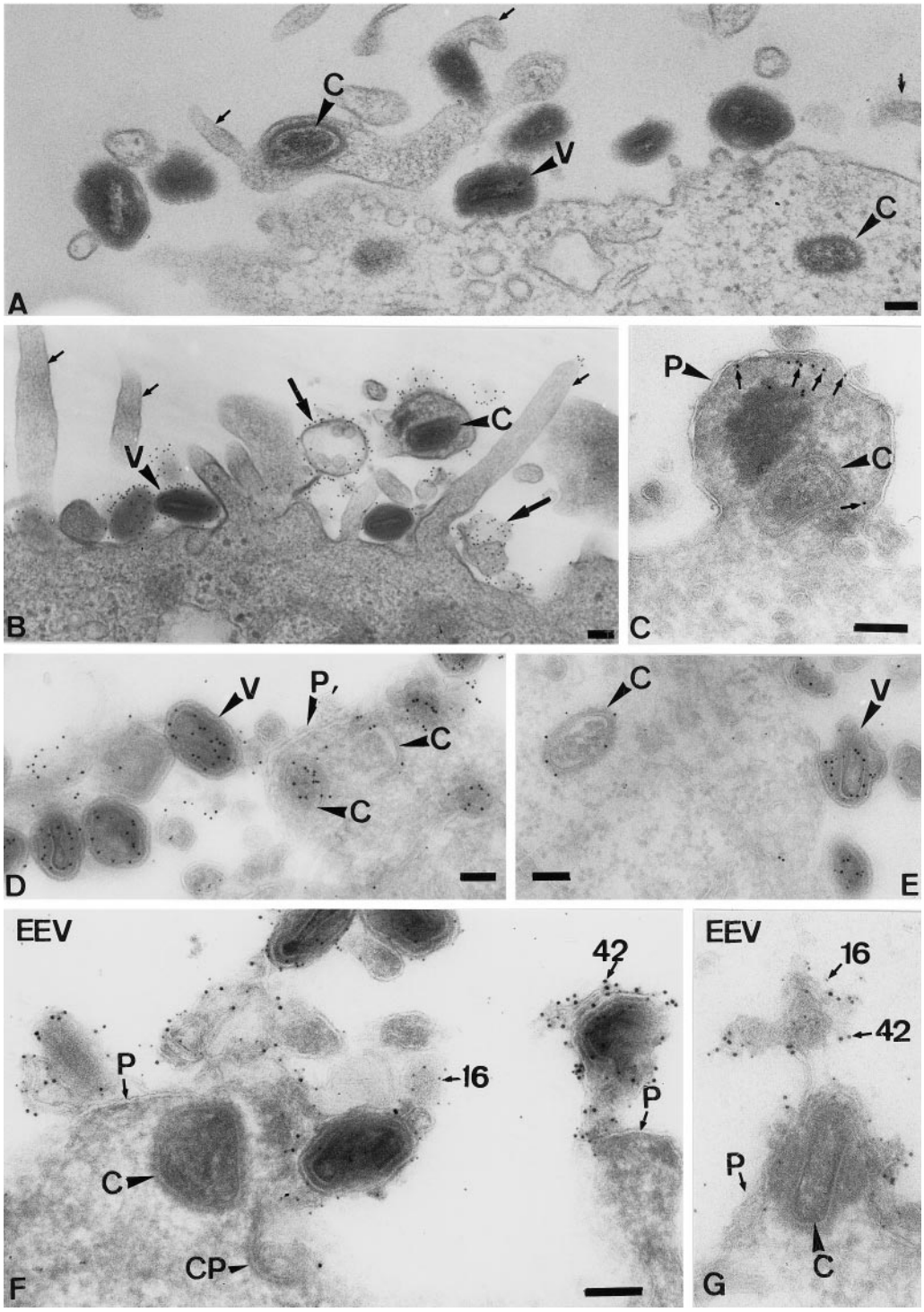

Figure 6. On entry, the IMV and EEV cores end up "free" in the cytoplasm, while the viral membranes remain at the plasma membrane. (A)–(E) HeLa cells were infected for 30 min at an MOI of 200 with IMV. (A) An Epon-embedded sample with intact virions (V) at the plasma membrane and cores (C) that are free in the cytoplasm. The *small arrows* indicate viral-induced projections; in one of those projections, a core can be seen that has apparently entered at the level of the microvillus. (B) Epon embedding after preembedding labeling with an antibody to the surface of the IMV. It shows several intact virions that label heavily. *Small arrows* indicate the microvilli induced by the virus. In the top right, a core has entered a microvillus (which seems to have enlarged), and material adjacent to the surrounding plasma membrane now heavily labels for the antibody to the viral membrane. The image also shows examples of labeled viral membranes (*large arrows*) devoid of cores that are not connected to the plasma membrane. (C)–(E) Cryosection of IMV-infected HeLa cells. (C) shows a swollen microvillus that contains a core (*large arrowhead*) that lies free in

Table 5. The effect of overexpression of dominant-negative or activated rho proteins and of full-length ezrin or ezrin 1-309 on IMV and EEV entry[a]

	IMV			EEV		
	Not transf.[b]	Transf.[c]	% of Contr.[d]	Not transf.[b]	Transf.[c]	% of Contr.[d]
V14RhoA	32.2 ± 10.2	9.4 ± 65.0	29	39.2 ± 12.6	35.3 ± 11.4	90
N19RhoA	42.5 ± 15.9	40.9 ± 19.8	100	46.1 ± 28.0	46.2 ± 22.0	100
L61rac1	32.6 ± 10.8	64.6 ± 25.9	200	39.2 ± 14.3	43.7 ± 15.8	110
N17rac1	35.1 ± 11.8	20.2 ± 11.1	58	37.8 ± 15.5	40.5 ± 15.3	107
L61CDC42	35.6 ± 14.0	33.9 ± 14.6	95	43.1 ± 20.7	41.8 ± 18.4	97
N17CDC42	33.3 ± 14.1	35.1 ± 12.3	105	40.4 ± 16.7	39.6 ± 16.8	100
Ezrin-fl	36.1 ± 17.2	36.1 ± 17.4	100	46.3 ± 16.0	45.8 ± 16.1	100
Ezrin-N	36.9 ± 17.1	54.4 ± 21.0	147	48.4 ± 27.8	50.5 ± 25.8	105

[a] IMV infection was at MOI 30 and EEV at MOI 10.

[b] Average number of cores and S.D.s in nontransfected HeLa cells. $N = 25 \pm$ S.D.s.

[c] Average number of cores and S.D.s in transfected cells (anti-*myc* or anti-P5D4 positive) with activated rhoA (V14 rhoA), rac1 (L61rac1), CDC42 (L61CDC42), dominant-negative rhoA (N19rhoA), rac1 (N17rac1), and CDC42 (N17CDC42), and full-length ezrin (ezrin-fl) or ezrin 1-309 (ezrin-N). $N = 25$.

[d] % of contr. indicates the percentage of inhibition or stimulation of entry on overexpression of the respective proteins compared to untransfected cells.

(EGF) had only marginal effects (25% increase; Table 6). In contrast, bombesin (which is known to activate rac1; Zigmond, 1996) stimulated the entry of the IMV by 50–60% (Table 6).

These data clearly implicate a role for the GTPase rac1 in the entry of the IMV in HeLa cells and suggest that perhaps rho might be antagonistic to rac.

Phosphorylation by Protein Kinase C May Be Part of the IMV Signaling Cascade

We attempted next to determine the events that might connect IMV-receptor activation to the activation of rac1 and/or ezrin. For this, HeLa cells were pretreated with various drugs that affect heterotrimeric G proteins, PI3kinase, protein kinase A and C, tyrosine phosphorylation, as well as phospholipase C. IMV entry was not affected by pertussis toxin, cholera toxin, or aluminum fluoride, arguing against a role for trimeric G proteins (Table 7). No inhibition was observed with wortmannin and U73122, implying that (most

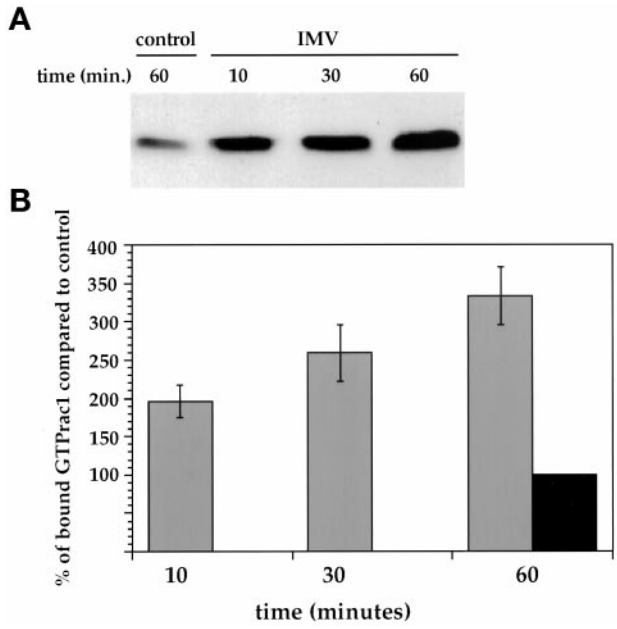

Figure 7. Exposure of HeLa cells to IMV leads to rac1 activation. (A) shows a representative Western blot of rac1-GTP levels in cell lysates that were either incubated for 60 min in serum-free DMEM (control) or for the indicated times in serum-free DMEM containing purified IMV at an MOI of 40 (IMV). Rac1-GTP was affinity isolated from cell lysates and was detected by ECL. (B) shows the quantitation of four independent experiments. Western blots were probed with antirac1 and antimouse ^{35}SLR, and the blots were quantified by phosphoimager. The average counts of uninfected cells incubated for 60 min in serum-free DMEM (black bar, 60 min) from four experiments was taken as 100%. The gray bars are from HeLa cells exposed to IMV for different periods of time.

Figure 6 (cont). the cytoplasm. The small arrows denote ezrin labeling. P, plasma membrane. (D) shows intact virions outside and cores inside the cell both labeled with anticore and clearly separated by the plasma membrane (P). E shows a cytoplasmic core and three virions at the plasma membrane labeled with anticore. The marked virion is clearly changing its morphology. We believe that this change is part of the (elusive) IMV entry mechanism. The section was double labeled with anticore (10-nm gold) and antip16 (5-nm gold). (F) and (G) Cryosections of cells infected with EEV for 10 min. The sections were double labeled for the IMV membrane protein p16 (5-nm gold) and the EEV membrane protein p42 (10-nm gold; both indicated). Whereas the core can be found in the cytoplasm underneath the cell surface, membrane fragments labeled for both p16 and p42 are found attached to the plasma membrane. CP, coated pit. Bars, 100 nm. (F) and (G) are the same magnification.

Table 6. The effect of ligands on IMV and EEV entry in serum-starved HeLa cells

Ligand[a]	IMV (%)	EEV (%)
Control	100[b]	100
S 1-P (1 μM)	33	100
Bombesin (100 nM)	155	100
EGF (50 ng/ml)	125	100
PDGF (5 ng/ml)	100	100
Bradikynin (100 ng/ml)	100	100

[a] Concentration of the ligand in nM, μM or ng/ml.

[b] The entry is expressed as a percentage of the control. The control (untreated cells) was taken as 100%. In each case, the cores in 30 serum-starved and treated or untreated cells were counted.

of the isoforms of) PI3 kinase or phospholipase C were also not involved (Table 7). Significant inhibition was, however, observed with the general kinase inhibitor staurosporin (61% at 200 nM), as well as the protein kinase C-inhibiting drugs calphostin C (70% at 250 nM) and bisindolylmaleimide (40% at 10 μM; Table 7), while a myristoylated peptide mimicking the active site of protein kinase A had no effect. When cells were treated for 10 min with phorbol 12-myristate 13-acetate (PMA), which is expected to activate PKC and consequently to increase IMV entry, the penetration of this latter virus was, on the contrary, inhibited by 50%.

The inhibition of IMV entry also was observed using two drugs that affect tyrosine phosphorylation (69% inhibition with genistein and 72% inhibition with tyrphostin 23; Table 7). None of these drugs significantly affected the entry of the EEV with the exception of the two tyrosine phosphorylation inhibitors that, at the highest concentration tested (200 μM for genistein and 100 μM for tyrphostin 23) affected its entry by $\sim$ 20% (Table 7).

Table 7. The effect of several drugs on IMV and EEV entry[a]

Drug concentration	Target	IMV (%)	EEV (%)
Pertussis toxin (500 ng/ml)	Trimeric G	100[b]	100[b]
Cholera toxin (500 ng/ml)	Trimeric G	100	100
Alf^{4-}	Trimeric G	100	100
Wortmannin (0.5 μM)	PI_3 kinase	100	100
PMA (100 nM)	PKC	50	100
Staurosporin (200 nM)	PK	39	100
Calphostin C (250 nM)	PKC	30	100
BIS (10 μM)	PKC	60	100
Genistein (25 μM)	PTK	65	100
Genistein (200 μM)	PTK	31	77
Tyrphostin 23 (25 μM)	PTK	57	100
Tyrphostin 23 (100 μM)	PTK	28	80
Myr. A (500 nM)	PKA	100	100
U73122 (20 μM)	PLC	100	100

[a] Target, the intracellular target of the drug; Trimeric G, trimeric G proteins; PKC, protein kinase C; PK, protein kinase; PTK, protein tyrosine kinase; PKA, protein kinase A; PLC, phospholipase C; Alf^{4-}, aluminium fluoride; PMA, phorbol 12-myristate 13-acetate; BIS, Bisindolylmaleimide; Myr. A, myristoylated peptide mimicking the active site of protein kinase A.

[b] In each case, 30 treated cells were counted and the amount is expressed as a percentage of the control, which consisted of untreated cells.

Table 8. The effect on IMV entry of staurosporin, calphostin C and tryphostin 23 on HeLa cells overexpressing L61rac1

Drug concentration	Nontransfected cells (%)	L61rac1 transfected cells (%)
Control	100[a]	100[b]
Staurosporin (100 nM)	55	88
Staurosporin (200 nM)	27.5	73
Calphostin C (200 nM)	34	89
Calphostin C (400 nM)	10	79
Tyrphostin 23 (50 μM)	31	39
Tyrphostin 23 (100 μM)	17	16

[a] The average number of cores in untreated and nontransfected cells was taken as 100%.

[b] The average number of cores in untreated and transfected cells was taken as 100%. In each case the cores in 25 cells were counted and the values are the average of two independent experiments.

To determine whether the phosphorylation events might act before or after rac1 activation, the effect of staurosporin, calphostin C, and tyrphostin 23 was subsequently tested on cells overexpressing activated rac1. Table 8 clearly illustrates that the overexpression of L61rac1 was able to largely overcome the inhibitory effect of staurosporin and calphostin C but not that of the tyrosine phosphorylation inhibitor tyrphostin 23.

These data suggest that phosphorylation by PKC may precede rac1 activation and that both events, together with actin assembly, act in concert during the entry of the IMV.

DISCUSSION

Although it is generally assumed that during the infection with both the IMV and the EEV the same vv core particle ends up in the cytoplasm, the present study shows that the mechanism of entry of the two infectious forms is fundamentally different. IMV entry requires actin, can be stimulated by constitutively activated rac1 as well as the N-terminal part of ezrin, while drugs that affect PKC and PTK inhibit its entry. None of the drugs or overexpressed proteins affected EEV entry, thus showing that the effects we describe for the IMV were specific and were not related to cytotoxic effects. The combined results thus represent the first example of an enveloped virus requiring actin and signaling for its entry in a manner similar to pathogenic bacteria.

Our data are consistent with the results of Payne and Norrby (1978) showing that the entry of the IMV, but not the EEV, was affected by cytochalasin B. Recent results by Vanderplasschen *et al.* (1998), however, suggested that the entry of both the IMV and the EEV was blocked by CD. The authors suggested that unpurified EEV taken straight from the medium entered cells differently from purified virus because the EEV-specific membrane might rupture during purification. Unfortunately, we were unable to reproduce

the entry assay described in that study, using unpurified and unconcentrated EEV. Purification in the present study was done using OptiPrep gradients instead of the standard sucrose or cesium chloride, resulting (as assessed by negative-staining EM) in 20–30% of EEVs with a partially opened EEV membrane. Nevertheless, throughout this study we show that our purified EEV behaved differently toward the IMV in almost every respect.

The present data show that the IMV activates a signaling cascade, leading to the formation of cell–surface protrusions that appear to be needed for the core to cross the plasma membrane. We assume that (unknown) viral receptors are the primary mediators of this response on IMV binding. Only one candidate receptor for the IMV has been described so far (Chung *et al.*, 1998), but because of the complexity of the particle and its wide host range, the IMV (as well as the EEV) is likely to use more than one receptor for entry. The simplest model for a signaling cascade that we can propose is that IMV binding induces concomitant activation of ERM proteins, tyrosine kinases, PKC, and rac1. The overexpression of activated rac1 was almost completely able to overcome the block in entry by PKC inhibitors, suggesting that a PKC-dependent event may be "upstream" of rac1. This observation is consistent with earlier data, showing that the activation of one of the nucleotide exchange factors for rac1, Tiam-1, can occur via phosphorylation by PCK (Fleming *et al.*, 1997).

The ERM proteins have been shown to become phosphorylated both on serine/threonines as well as on tyrosine residues, and these modifications are most likely linked to their activation (Bretscher, 1999; Mangeat *et al.*, 1999). In their dormant state, the N-terminus of ERM proteins binds "head-to-tail" to the C-terminus, an association that is lost on activation. The free termini then become available for interaction with themselves to form dimers or to interact with other molecules at the membrane. EGF receptor activation (possibly via rac1) may be linked to tyrosine phosphorylation of ERM proteins and to subsequent plasma membrane ruffling (Bretscher, 1989; Krieg and Hunter, 1992; Ridley *et al.*, 1992; Bretscher and Aguado-Velasco, 1998), providing a possible explanation for the fact that IMV entry was decreased by inhibitors of tyrosine phosphorylation. ERM proteins also have been extensively linked to the rho protein family (Hirao *et al.*, 1996; Kotani *et al.*, 1997; Mackay *et al.*, 1997; Takahashi *et al.*, 1997; Matsui *et al.*, 1998; Shaw *et al.*, 1998). They can bind directly to RhoGDI (Takahashi *et al.*, 1997) as well as to the Rho GDP/GTP exchange factor Dbl (Takahashi *et al.*, 1998), suggesting that ERM may activate Rho proteins. In vitro RhoGDI has been shown to bind the ERM N-terminus but not the full-length (folded) molecule (Takahashi *et al.*, 1997), providing a possible explanation for why overexpression of ezrin 1–309 stimulated IMV entry; by binding more rhoGDI, the overexpressed protein could activate rho family proteins.

The IMV seemed to require activated rac1 for its entry, while activated rhoA inhibited this process. One possibility is therefore that activated rhoA antagonized the function of rac1 (see Schoenwaelder and Burridge, 1999). Alternatively, the effect of V14rhoA on IMV entry might be indirect; the overexpression of activated rhoA induces exaggerated amounts of stress fibers, which may result in less G actin being available for polymerization at the plasma membrane, as suggested by Ridley *et al.* (1995).

The available data on vv entry have been interpreted as showing that vv enters cells by a fusion process at the plasma membrane (Armstrong *et al.*, 1973; Granados, 1973; Chang and Metz, 1976). In a separate study, we have accumulated extensive data arguing against a conventional fusion process (Krijnse Locker *et al.*, unpublished results). Both with the IMV and the EEV we observed a separation of the viral membranes and membrane proteins from the core at the point of entry, while the cores, after crossing the plasma membrane barrier, end up free in the adjacent cytoplasm. That this mechanism does not involve fusion is most dramatically exemplified by the fact that none of the viral membrane proteins appear to be implanted into the plasma membrane, as would be expected for a fusion event (Krijnse Locker *et al.*, unpublished results).

Although morphologically the process of entry appears very similar for the two viral forms, the entry is in other respects quite different, since the IMV signals to the cells and the EEV does not. We speculate that the actin–membrane rearrangements induced by the IMV are similar to the initial stages of phagocytosis, since the IMV, in principle, is large enough ($>$ 0.3 μm) to evoke a phagocytic response. However, since from our morphological data the IMV is not internalized into HeLa cells into a phagosome, the reasons why this virus needs to induce the formation of actin-containing protrusions at the plasma membrane for its entry remain open. Obvious possibilities are that the microvillar-like structures concentrate or expose a new domain of the (outer leaflet of the) plasma membrane that is enriched in lipids and/or proteins that facilitate binding or entry of the IMV core.

The acquisition of an additional membrane containing six known membrane proteins enables the EEV to enter cells in an apparent "silent" way. Since the surface of the EEV exposes an entirely different set of proteins, the most obvious explanation for this difference is that this virus binds different putative receptors (see Vanderplasschen *et al.*, 1998) that do not lead to cell activation. Perhaps the EEV is capable of locking its receptor(s) in a manner that prevents oligimerization, usually an essential prelude to signaling.

An important fact to consider is that, although during infection significantly more IMV than EEV is made (see Introduction), the latter virus is the major player in cell-to-cell spread and in disease transmission. The fact that the EEV is capable of entry without signaling could give it an important immunological advantage over the IMV in being able to enter without (initially) activating potential cellular defense mechanisms. Clearly, these speculations now need to be tested experimentally.

ACKNOWLEDGMENTS

The following people are acknowledged for providing us with reagents: Christian Roy and Paul Mangeat, Alan Hall, Tyler Jacks, Dr. Gabianni, Monique Arpin, Shubda Bagrodia, and Becky Worthylake. We would like to thank Marino Zerial for advice and Kai Simons for critical reading of the manuscript. We dedicate this article to the two new Zerials, who have just joined us.

REFERENCES

Adam, T., Giry, M., Boquet, P., and Sansonetti, P. (1996). Rho-dependent membrane folding causes *Shigella* entry into epithelial cells. EMBO J. *15*, 3315–3321.

Algrain, M., Turunen, O., Vaheri, A., Louvard, D., and Arpin, M. (1993). Ezrin contains cytoskeleton and membrane binding domains accounting for its proposed role as a membrane-cytoskeleton linker. J. Cell. Biol. *120*, 129–139.

Armstrong, J.A., Metz, D.H., and Young, M.R. (1973). The mode of entry of vaccinia virus into L cells. J. Gen. Virol. *21*, 533–537.

Ayscough, K. (1998). Use of latrunculin-A, an actin monomer-binding drug. Methods Enzymol. *298*, 18–25.

Bagrodia, S., Taylor, S.J., Jordon, K.A., Van Aelst, L., and Cerione, R.A. (1998). A novel regulator of p21-activated kinases. J. Biol. Chem. *273*, 23633–23636.

Blasco, R., and Moss, B. (1991). Extracellular vaccinia virus formation and cell-to-cell virus transmission are prevented by a deletion of the gene encoding the 37,000-dalton outer envelope protein. J. Virol. *65*, 5910–5920.

Bretscher, A. (1989). Rapid phosphorylation and reorganization of ezrin and spectrin accompany morphological changes induced in A-431 cells by epidermal growth factor. J. Cell. Biol. *108*, 921–930.

Bretscher, A. (1999). Regulation of cortical structure by the ezrin-radixin-moesin protein family. Curr. Opin. Cell. Biol. *11*, 109–116.

Bretscher, M.S., and Aguado-Velasco, C. (1998). EGF induces recycling membrane to form ruffles. Curr. Biol. *8*, 721–724.

Bubb, M.R., Senderowicz, A.M., Sausville, E.A., Duncan, K.L., and Korn, E.D. (1994). Jasplakinolide, a cytotoxic natural product, induces actin polymerization and competitively inhibits the binding of phalloidin to F-actin. J. Biol. Chem. *269*, 14869–14871.

Chang, A., and Metz, D.H. (1976). Further investigations on the mode of entry of vaccinia virus into cells. J. Gen. Virol. *32*, 275–282.

Chen, L.-M., Hobbie, S., and Galan, J.E. (1996). Requirement of CDC42 for *Salmonella*-induced cytoskeleton and nuclear responses. Science *274*, 2115–2118.

Chung, C.S., Hsiao, J.C., Chang, Y.S., and Chang, W. (1998). A27L protein mediates vaccinia virus interaction with cell surface heparan sulfate. J. Virol. *72*, 1577–1585.

Cooper, J.A. (1987). Effects of cytochalasin and phalloidin on actin. J. Cell. Biol. *105*, 1473–1478.

Crepaldi, T., Gautreau, A., Comoglio, P.M., Louvard, D., and Arpin, M. (1997). Ezrin is an effector of hepatocyte growth factor-mediated migration and morphogenesis in epithelial cells. J. Cell. Biol. *138*, 423–434.

Cudmore, S., Cossart, P., Griffiths, G., and Way, M. (1995). Actin-based motility of vaccinia virus. Nature *378*, 636–638.

Cudmore, S., Blasco, R., Vincentelli, R., Esteban, M., Sodeik, B., Griffiths, G., and Krijnse Locker, J. (1996). A vaccinia virus core protein, p39, is membrane associated. J. Virol. *70*, 6909–6921.

Dales, S., and Kajioka, R. (1964). The cycle of multiplication of vaccinia virus in Earle's strain L cells. 1. Uptake and penetration. Virology *24*, 278–294.

Den Boon, J.A., Snijder, E.J., Krijnse Locker, J., Horzinek, M.C., and Rottier, P.J.M. (1991). Another triple-spanning envelope protein among intracellular budding RNA viruses: the torovirus E protein. Virology *182*, 655–663.

Doms, R.W., Blumenthal, R., and Moss, B. (1990). Fusion of intra- and extracellular forms of vaccinia virus with the cell membrane. J. Virol. *64*, 4884–4892.

Dramsi, S., and Cossart, P. (1998). Intracellular pathogens and the actin cytoskeleton. Annu. Rev. Cell. Dev. Biol. *14*, 137–166.

Ericsson, M., Cudmore, S., Shuman, S., Condit, R.C., Griffiths, G., and Krijnse Locker, J. (1995). Characterization of ts 16, a temperature sensitive mutant of vaccinia virus. J. Virol. *69*, 7072–7086.

Essani, K., and Dales, S. (1979). Biogenesis of vaccinia: evidence for more than 100 polypeptides in the virion. Virology *95*, 385–394.

Finlay, B.B., and Cossart, P. (1997). Exploitation of mammalian host cell functions by bacterial pathogens. Science *276*, 718–25.

Fleming, I.N., Elliott, C.M., Collard, J.G., and Exton, J.H. (1997). Lysophosphatidic acid induces threonine phosphorylation of Tiam1 in Swiss 3T3 fibroblasts via activation of protein kinase C. J. Biol. Chem. *272*, 33105–33110.

Galan, J.E. (1996). Molecular and cellular bases of *Salmonella* entry into host cells. Curr. Top. Microbiol. Immunol. *209*, 43–60.

Gottlieb, T.A., Ivanov, I.E., Adesnik, M., and Sabatini, D.D. (1993). Actin microfilament play a critical role in endocytosis at the apical but not basolateral surface of polarized epithelial cells. J. Cell. Biol. *120*, 695–710.

Granados, R.R. (1973). Entry of an insect poxvirus by fusion of the virus envelope with the host cell membrane. Virology *52*, 305–309.

Hall, A. (1998). Rho GTPases and the actin cytoskeleton. Science *279*, 509–514.

Hauck, C.R., Meyer, T.F., Lang, F., and Gulbins, E. (1998). CD66-mediated phagocytosis of Opa52 *Neisseria* gonorrhoeae requires a Src-like tyrosine kinase- and rac1-dependent signaling pathway. EMBO J. *17*, 443–454.

Hirao, M., Sato, N., Kondo, T., Yonemura, S., Monden, M., Sasaki, T., Takai, Y., Tsukita, S., and Tsukita, S. (1996). Regulation mechanism of ERM (ezrin/radixin/moesin) protein/plasma membrane association: possible involvement of phosphatidylinositol turnover and Rho-dependent signaling pathway. J. Cell. Biol. *135*, 37–51.

Hohenberg, H. (1989). Replica preparation techniques in immunogold cytochemistry. In: Immuno-Gold Labeling in Cell Biology, ed. A. Verkleij, Boca Raton, FL: CRC Press, 157–177.

Hollinshead, M., Vanderplasschen, A., Smith, G.L., and Vaux, D.J. (1999). Vaccinia virus intracellular mature virions contain only one lipid membrane. J. Virol. *73*, 1503–1517.

Holzinger, A., and Meindl, U. (1997). Jasplakinolide, a novel actin targeting peptide, inhibits cell growth and induces actin filament polymerization in the green alga Micrasterias. Cell. Motil. Cytoskeleton *38*, 365–372.

Iyengar, S., Hildreth, J.E.K., and Schwartz, D.H. (1998). Actin-dependent receptor colocalization required for human immunodeficiency virus entry into host cells. J. Virol. *72*, 5251–5255.

Jensen, O.N., Houthaeve, T., Shevchenko, A., Cudmore, S., Mann, M., Griffiths, G., and Krijnse Locker, J. (1996). Identification of the major membrane and core proteins of vaccinia virus by two-dimensional electrophoresis. J. Virol. *70*, 7485–7497.

Kielian, M., and Jungerwirth, S. (1990). Mechanisms of enveloped virus entry into cells. Mol. Biol. Med. *7*, 17–31.

Kizhatil, K., and Albritton, L.M. (1997). Requirements for different components of the host cell cytoskeleton distinguish ecotropic murine leukemia virus entry via endocytosis from entry via surface fusion. J. Virol. *71*, 7145–7156.

Kotani, H., Takaishi, K., Sasaki, T., and Takai, Y. (1997). Rho regulates association of both the ERM family and vinculin with the plasma membrane in MDCK cells. Oncogene *14*, 1705–1713.

Krieg, J., and Hunter, T. (1992). Identification of the two major epidermal growth factor-induced tyrosine phosphorylation sites in the microvillar core protein ezrin. J. Biol. Chem. *267*, 19258–19265.

Krijnse Locker, J., and Griffiths, G. (1999). An unconventional role for cytoplasmic disulfide bonds in vaccinia virus proteins. J. Cell. Biol. *144*, 267–279.

Mackay, D.J., Esch, F., Furthmayr, H., and Hall, A. (1997). Rho- and rac-dependent assembly of focal adhesion complexes and actin filaments in permeabilized fibroblasts: an essential role for ezrin/radixin/moesin proteins. J. Cell. Biol. *138*, 927–938.

Mangeat, P., Roy, C., and Martin, M. (1999). ERM proteins in cell adhesion and membrane dynamics. Trends Cell Biol. *9*, 187–192.

Marsh, M., and Helenius, A. (1989). Virus entry into animal cells. Adv. Virus Res. *36*, 107–151.

Martin, M., Andreoli, C., Sahuquet, A., Montcourrier, P., Algrain, M., and Mangeat, P. (1995). Ezrin NH_2-terminal domain inhibits the cell extension activity of the COOH-terminal domain. J. Cell. Biol. *128*, 1081–1093.

Martin, M., Roy, C., Montcourrier, P., Sahuquet, A., and Mangeat, P. (1997). Three determinants in ezrin are responsible for cell extension activity. Mol. Biol. Cell. *8*, 1543–1557.

Matsui, T., Maeda, M., Doi, Y., Yonemura, S., Amano, M., Kaibuchi, K., Tsukita, S., and Tsukita, S. (1998). Rho-kinase phosphorylates COOH-terminal threonines of ezrin/radixin/moesin (ERM) proteins and regulates their head-to-tail association. J. Cell Biol. *140*, 647–657.

Menard, R., Dehio, C., and Sansonetti, P.J. (1996). Bacterial entry into epithelial cells: the paradigm of *Shigella*. Trends Microbiol. *4*, 220–226.

Moss, B. (1990). Poxviridae and their replication. In: Fields Virology, eds. B.N. Fields, D.M. Knipe, R.M. Chanock, M.S. Hirsch, J.L. Melnick, T.P. Monath, and B. Roizman, New York: Raven Press, 2079–2111.

Mounier, J., Laurent, V., Hall, A., Fort, P., Carlier, M.-F., Sansonetti, P.J., and Egile, C. (1999). Rho family GTPases control entry of *Shigella flexneri* into epithelial cells but not intracellular motility. J. Cell Sci. *112*, 2069–2080.

Payne, L.G., and Norrby, E. (1978). Adsorption and penetration of enveloped and naked vaccinia virus particles. J. Virol. *27*, 19–27.

Payne, L.G. (1978). Polypeptide composition of extracellular enveloped vaccinia virus. J. Virol. *27*, 28–37.

Payne, L.G. (1980). Significance of extracellular enveloped virus in the in vitro and in vivo dissemination of vaccinia. J. Gen. Virol. *50*, 89–100.

Pedersen, K., Snijder, E., Schleich, S., Roos, N., Griffiths, G., and Krijnse Locker, J. (2000). Characterization of vaccinia virus intracellular cores: implications for viral uncoating and core structure. J. Virol. *74*, 3525–3536.

Ridley, A.J., Comoglio, P.M., and Hall, A. (1995). Regulation of scatter factor/hepatocyte growth factor responses by ras, rac, and rho in MDCK cells. Mol. Cell. Biol. *15*, 1110–1122.

Ridley, A.J., Paterson, H.F., Johnston, C.L., Diekmann, D., and Hall, A. (1992). The small GTP-binding protein rac regulates growth factor-induced membrane ruffling. Cell *70*, 401–410.

Ritter, M., Henry, D., Wiesner, S., Pfeiffer, S., and Wepf, R. (1999). A versatile high-vacuum cryo-transfer for cryo-FESEM, cryo-SPM and other imaging techniques. *in* Microsc. Microanal. *5*(suppl), 1–5.

Rodriguez, D., Esteban, M., and Rodriguez, J.R. (1995). Vaccinia virus A17L gene product is essential for an early step in virion morphogenesis. J. Virol. *69*, 4640–4648.

Roper, R.L., Payne, L.G., and Moss, B. (1996). Extracellular vaccinia virus envelope glycoprotein encoded by the A33R gene. J. Virol. *70*, 3753–3762.

Rosenthal, K.S., Perez, R., and Hodnichak, C. (1985). Inhibition of herpes simplex virus type 1 penetration by cytochalasins B and D. J. Gen. Virol. *66*, 1601–1605.

Salmons, T., Kuhn, A. Wylie, F., Schleich, S., Rodriguez, J.R., Rodriguez, D., Esteban, M., Griffiths, G., and Krijnse Locker, J. (1997). Vaccinia virus membrane proteins p8 and p16 are co-translationally inserted into the rough ER and retained in the intermediate compartment. J. Virol. *71*, 7404–7420.

Schmelz, M., Sodeik, B., Ericsson, M., Wolffe, E., Shida, H., Hiller, G., and Griffiths, G. (1994). Assembly of vaccinia virus: the second wrapping cisterna is derived from the trans Golgi network. J. Virol. *68*, 130–147.

Shaw, R.J., Henry, M., Solomon, F., and Jacks, T. (1998). RhoA-dependent phosphorylation and relocalization of ERM proteins into apical membrane/actin protrusions in fibroblasts. Mol. Biol. Cell *9*, 403–419.

Schoenwaelder, S.M., and Burridge, K. (1999). Bidirectional signaling between the cytoskeleton and integrins. Curr. Opin. Cell Biol. *11*, 274–286.

Skoudy, A., Van Nhieu, G.T., Mantis, N., Arpin, M., Mounier, J., Gounon, P., and Sansonetti, P. (1999). A functional role for ezrin during *Shigella flexneri* entry into epithelial cells. J. Cell. Sci. *112*, 2059–2068.

Sodeik, B., Doms, R.W., Ericsson, M., Hiller, G., Machamer, C.E., van't Hof, W., van Meer, G., Moss, B., and Griffiths, G. (1993). Assembly of vaccinia virus: role of the intermediate compartment between the endoplasmic reticulum and the Golgi stacks. J. Cell Biol. *121*, 521–541.

Takahashi, K., Sasaki, T., Mammoto, A., Takaishi, K., Kameyama, T., Tsukita, S., Tsukita, S., and Takai, Y. (1997). Direct interaction of the Rho GDP dissociation inhibitor with ezrin/radixin/moesin initiates the activation of the rho small G protein. J. Biol. Chem. *272*, 23371–23375.

Takahashi, K., Sasaki, T., Mammoto, A., Hotta, I., Takaishi, K., Imamura, H., Nakano, K., Kodama, A., and Takai, Y. (1998). Interaction of radixin with rho small G protein GDP/GTP exchange protein Dbl. Oncogene *16*, 3279–3284.

Tsukita, S., and Yonemura, S. (1997). ERM (ezrin/radixin/moesin) family: from cytoskeleton to signal transduction. Curr. Opin. Cell Biol. *9*, 70–75.

van der Meer, Y., Snijder, E.J., Dobbe, J.C., Schleich, S., Denison, M.R., Spaan, W.J.M., and Krijnse Locker, J. (1999). The localization of mouse hepatitis virus nonstructural proteins and RNA synthesis indicates a role for late endosomes in viral replication. J. Virol.*73*, 7641–7657.

Vanderplasschen, A., and Smith, G.L. (1997). A novel binding assay using confocal microscopy: demonstration that the intracellular and extracellular vaccinia virions bind to different cellular receptors. J. Virol. *71*, 4032–4041.

Vanderplasschen, A., Hollinshead, M., and Smith, G.L. (1998). Intracellular and extracellular vaccinia virions enter cells by different mechanisms. J. Gen. Virol. *79*, 877–887.

Watarai, M., Kamata, Y., Kozaki, S., and Sasakawa, C. (1997). Rho, a small GTP-binding protein, is essential for *Shigella* invasion of epithelial cells. J. Exp. Med. *185*, 281–292.

Waterman-Storer, C.M., Worthylake, R.A., Liu, B.P., Burridge, K., and Salmon, E.D. (1999). Microtubule growth activates rac1 to promote lamellipodial protrusion in fibroblasts. Nat. Cell Biol. *1*, 45–50.

Wolffe, E.J., Moore, D.M., Peters, P.J., and Moss, B. (1996). Vaccinia virus A17L open reading frame encodes an essential component of nascent viral membranes that is required to initiate morphogenesis. J. Virol. *70*, 2797–2808.

Zigmond, S.H. (1996). Signal transduction and actin filament organization. Curr. Opin. Cell Biol. *8*, 66–73.